Conserved transcriptional programming across sex and species after peripheral nerve injury predicts treatments for neuropathic pain

Shahrzad Ghazisaeidi[1], Milind Muley[2], YuShan Tu[2], Mahshad Kolahdouzan[1], Ameet Sengar[2], Arun Ramani[3], Michael Brudno[1], and Michael Salter[1]

[1]University of Toronto
[2]Hospital for Sick Children Research Institute
[3]Hospital For Sick Children

September 15, 2022

Abstract

Background and Purpose: Chronic pain is a devastating problem affecting 1 in 5 individuals around the globe, with neuropathic pain the most debilitating and poorly treated type of chronic pain. Advances in transcriptomics and data mining have contributed to cataloging diverse cellular pathways and transcriptomic alterations in response to peripheral nerve injury but have focused on phenomenology and classifying transcriptomic responses. **Experimental approach:** Here, with the goal of identifying new types of pain-relieving agents, we compared transcriptional reprogramming changes in the dorsal spinal cord after peripheral nerve injury cross-sex and cross-species and imputed commonalities, as well as differences in cellular pathways and gene regulation. **Key Results**: We identified 93 transcripts in the dorsal horn that were increased by peripheral nerve injury in male and female mice and rats. Following gene ontology and transcription factor analyses, we constructed a pain interactome for the proteins encoded by the differentially expressed genes, discovering new, conserved signaling nodes. We interrogated the interactome with the Drug-Gene database to predict FDA-approved medications that may modulate key nodes within the network. The top hit from the analysis was fostamatinib, the molecular target of which is the non-receptor tyrosine kinase Syk, which our analysis had identified as a key node in the interactome. **Conclusions & Implications :** We found that intrathecally administrating the active metabolite of fostamatinib, R406, significantly reversed pain hypersensitivity in both sexes. Thus, we have identified and shown the efficacy of an agent that could not have been previously predicted to have analgesic properties.

Title: Conserved transcriptional programming across sex and species after peripheral nerve injury predicts treatments for neuropathic pain

One sentence summary: Unbiased approach to predicting safe therapies for neuropathic pain

Authors: Shahrzad Ghazisaeidi[1,2], Milind M. Muley[2], YuShan Tu[2], Mahshad Kolahdouzan[1,2], Ameet S. Sengar[2], Arun K. Ramani[3], Michael Brudno[3,4], Michael W. Salter [1,2*]

Affiliations:

[1]Department of Physiology, University of Toronto; Toronto, Canada.

[2]Program in Neuroscience & Mental Health, Hospital for Sick Children; Toronto, Canada.

[3]Centre for Computational Medicine, Hospital for Sick Children; Toronto, Canada.

[4]Department of Computer Science, University of Toronto; Toronto, Canada.

*Corresponding Author: Michael W. Salter, Hospital for Sick Children, 686 Bay Street, Toronto, Canada, M5G 0A4. Email: michael.salter@sickkids.ca

Competing Interests Statement : none
Data Availability Statement: Data available on request from the authors
**** RNA-seq data will be openly shared with the public upon publication; authors can provide tokens from GEO database for reviewers to access the raw data upon request.**

Abstract

Background and Purpose

Chronic pain is a devastating problem affecting 1 in 5 individuals around the globe, with neuropathic pain the most debilitating and poorly treated type of chronic pain. Advances in transcriptomics and data mining have contributed to cataloging diverse cellular pathways and transcriptomic alterations in response to peripheral nerve injury but have focused on phenomenology and classifying transcriptomic responses.

Experimental approach

Here, with the goal of identifying new types of pain-relieving agents, we compared transcriptional reprogramming changes in the dorsal spinal cord after peripheral nerve injury cross-sex and cross-species and imputed commonalities, as well as differences in cellular pathways and gene regulation.

Key Results

We identified 93 transcripts in the dorsal horn that were increased by peripheral nerve injury in male and female mice and rats. Following gene ontology and transcription factor analyses, we constructed a pain interactome for the proteins encoded by the differentially expressed genes, discovering new, conserved signalling nodes. We interrogated the interactome with the Drug-Gene database to predict FDA-approved medications that may modulate key nodes within the network. The top hit from the analysis was fostamatinib, the molecular target of which is the non-receptor tyrosine kinase Syk, which our analysis had identified as a key node in the interactome.

Conclusions & Implications

We found that intrathecally administrating the active metabolite of fostamatinib, R406, significantly reversed pain hypersensitivity in both sexes. Thus, we have identified and shown the efficacy of an agent that could not have been previously predicted to have analgesic properties.

Keywords: Peripheral Nerve Injury, Transcriptomic, Spinal cord, therapy

INTRODUCTION

Chronic pain affects 16-22% of the population and is one of the major silent health crises affecting physical and mental health (*1, 2*). Neuropathic pain, which results from damage to the somatosensory system in the peripheral or in the central nervous system (CNS) (*3*), is the most recalcitrant type of chronic pain. Therapeutic options for neuropathic pain are limited by poor efficacy, side effects, and tolerability of even approved pain medications (*4, 5*).

Damage to peripheral nerves is known to produce persistent functional reorganization of the somatosensory system in the CNS (*6*). The primary afferent neurons in peripheral nerves project into the dorsal horn of the spinal cord, which is the critical first site in the CNS for integrating, processing, and transmitting pain information. Transcriptomic changes in the dorsal horn produced by peripheral nerve injury have been increasingly described (*7-10*) with a large emphasis on characterizing sex differences in changes in gene expression. Such studies are touted to hold promise to characterize pathological biochemical pathways that might in the future reveal targets for new therapies. However, there has been a focus on cataloging transcriptomic changes, unconnected from identifying pain therapeutics. Thus, there remains a gap between describing molecular changes in the dorsal horn and identifying new therapeutics.

Here, we took on the challenge of filling this gap by using a purposeful approach to explore the possibility of identifying pain-relieving drugs in an unbiased way through connecting transcriptomic changes to drug discovery. To gain power in our study we simultaneously looked not just between sexes in a single species but between sexes in two species. Unexpectedly, given the growing prominence of sex differences across biomedical sciences, we found many more commonalities than differences between sexes and across species in the gene expression changes produced in the spinal dorsal horn ipsilateral to the peripheral nerve injury. From the

72 commonalities, we built a species-conserved sex-conserved pain interactome network. With an
73 unsupervised approach, we used this interactome to predict safe therapies that may have the most
74 impact.

75

76 **RESULTS**

77 We evaluated dorsal horn transcriptomes after spared nerve injury (SNI), a widely used model of
78 peripheral neuropathic pain (*11*), or sham surgery in male and female mice and rats, seven days
79 surgery (Fig. 1A). We collected gray matter from the dorsal horn of L4-L5 spinal cord ipsilateral
80 and contralateral to the surgery. In order to obtain sufficient RNA from mice, each sample was
81 pooled from two animals. The experimenters who did the dissections, tissue removal and
82 extraction of the RNA were unaware of which animals had undergone SNI or sham surgery.

83

84 **Dorsal horn transcriptomes ipsilateral to SNI form a distinct cluster**

85 To define main sources of transcriptome variability we first analyzed the datasets at the sample
86 level by principal component analysis separately for mice and for rats. In the mouse dataset, the
87 two principal components (PCs) PC1 (39%) and PC2 (22%) were the major PCs, explaining 61%
88 of the overall variance (fig. S1). We found in both males and females that there was a clear
89 clustering of the samples from the ipsilateral dorsal horn of animals that had received SNI
90 (SNI_ipsi) as compared to the remaining groups – contralateral to SNI (SNI_contra), ipsilateral
91 to sham surgery (Sham_ipsi), and contralateral to the sham (Sham_contra) (Fig. 1B). In the rat
92 dataset, two principal components explained 48% and 20% of the variance and SNI_ipsi samples
93 were distinct from the remainder (Fig. 1C). Thus, in both species there is a clear cluster

94 primarily across PC1 of SNI_ipsi samples separate from Sham_contra, Sham_ipsi and
95 SNI_contra.

96 In order to identify differentially expressed genes (DEGs) we did pairwise comparisons
97 between samples of the levels of individual genes. DEGs were defined with the criteria of the
98 adjusted P-value <0.01 and $\log_2$ fold-change absolute value greater than 0.5 (|log FC|> 0.5). In
99 comparing SNI_ipsi to the other groups we found numerous DEGs (fig. S2) whereas no DEGs
100 were detected comparing Sham_ipsi versus Sham_contra within sex and species (Fig. 1D).
101 Furthermore, there were no DEGs comparing SNI_contra compared with Sham_contra (Fig. 1E)
102 or with Sham_ipsi (Fig. 1F). Taking these findings together we conclude from both principal
103 component analysis and DEG analyses that the transcriptomes of the dorsal horn ipsilateral to
104 SNI are distinct from those contralateral to SNI or either of the sham groups. Moreover, because
105 we found no differences at the gene expression level in SNI_contra, Sham_ipsi and
106 Sham_contra, we combined these groups, by sex or by species, as comparators for the remainder
107 of our analyses (Fig. 1G).

108

109 **High correlation in the gene expression pattern of spinal cord dorsal horn in male and**
110 **female mice and rats after peripheral nerve injury**

111 From this analysis, we compared gene expression levels by sex and by species in the ipsilateral
112 dorsal horn after SNI with those in the respective comparator group (Fig. 2A-D). In mice we
113 observed that after SNI there was increased expression of 278 and 136 genes in males and
114 females, respectively (Fig. 2A, B). In females we found 14 genes expression of which was
115 significantly decreased after SNI where none was decreased in males (Fig. 2A, B & fig. S3). In
116 rats, 271 genes were upregulated in the SNI_ipsi males versus the comparator group and none

117 was decreased. Whereas in females, the expression level of 403 genes was increased, and that of
118 13 genes was decreased, after SNI (Fig. 2C-D & fig. S3). Thus, in both mice and rats
119 downregulation of gene levels after SNI was only observed in females, and of these DEGs there
120 were 4 in common in both species.

121 For genes that were differentially expressed after SNI in mice we compared the change in
122 the level of expression in males versus females (Fig. 2E) and found that the change in expression
123 level in females was highly positively correlated with that in males ($R_{pearson}$=0.68, $p<2.2*10^{-16}$).
124 As in mice, the expression levels of SNI-evoked DEGs in male and female rats showed a
125 significant positive correlation ($R_{pearson}$=0.96, $p<2.2*10^{-16}$, Fig. 2F). Moreover, by comparing
126 mice and rat datasets we found that gene expression changes were significantly correlated
127 between the two species ($R_{pearson}$=0.83, $p<2.2*10^{-16}$, Fig. 2G). Taking these findings together we
128 conclude that transcriptional reprograming in response to peripheral nerve injury is significantly
129 conserved in both sexes and in both species.

130

131 **Validation of combined analysis by sex and species**

132 Focusing on the genes that were differentially expressed in males and females of both species we
133 detected 93 DEGs increased in SNI_ipsi vs comparators (Fig. 3 A-B and table S1). In separate
134 cohorts of animals, the validity of the RNA sequencing was tested in four of these DEGs: three
135 of these had not been previously linked to neuropathic pain (Rasal3, Ikzf1, and Slco2b1) and for
136 P2ry12 (Table 1) which had been linked (*12*). For each of genes the relative expression level
137 measured by qPCR did not differ across sex or species (fig. S4A) and there was statistically
138 significant correlation between the relative expression level measured by qPCR and that by
139 RNAseq (fig. S4B).

140 The function of the 93 commonly upregulated genes was examined though Gene
141 Ontology (GO) analysis (table S2). We found significant enrichment (false discovery rate (FDR)
142 <0.05) of 26 biological processes of which 21 are directly related to immune responses (Fig. 3C).
143 The predominant cellular components defined by GO analysis were related to membranes and
144 those of GO molecular function were related to protein binding and G-protein coupled purinergic
145 nucleotide receptor activity (Fig. 3C). To interrogate cell-type specificity for the common
146 DEGs, we deconvolved the bulk RNA-seq dataset with scMappR (*13*) which uses publicly
147 available single cell-RNAseq data from the Panglao database (*14*). Deconvolution analysis (Fig.
148 3D and table S3) revealed five cell types with FDR less than 0.05 with the top three being
149 microglia cells (FDR=$6.7*10^{-19}$, Odds Ratio= 20.1), macrophages (FDR= $5.1*10^{-12}$, Odds Ratio=
150 13.9), and monocytes (FDR= $15.8 *10^{-5}$, Odds Ratio= 8.56).

151 In exploring possible sex differences in the transcriptome changes induced by SNI we
152 found 30 genes that were differentially expressed in female mice but not in males of either
153 species and 117 genes that were differentially expressed in female rats but not in males (Fig. 3B).
154 Of those female-specific DEGs four were common to females of both species including genes
155 encoding neurofilaments light (Nefl), medium (Nefm) and heavy (Nefh) polypeptide and
156 Proline-Serine-Threonine Phosphatase Interacting Protein 1 (Pstpip1). Notably, all of these
157 genes were decreased following SNI. Gene ontology analysis and single-cell deconvolution for
158 female mice and for female rats (fig. S5) revealed that while the individual transcripts differed
159 there was a pattern common in both species that these DEGs were expressed in neurons. For
160 males 87 genes were differentially expressed in male mice but not in females of either species
161 one sex or species and we observed 9 genes that were differentially expressed in male rats but
162 not in female rodents (Fig. 3B).

163 Together, the gene ontology analysis of the DEGs shows a pattern, biological processes,
164 functions, cellular components, and cell types, converging on microglia and immune response
165 pathways in the dorsal horn ipsilateral to the nerve injury in both sexes and species, and at the
166 same time the analysis reveals a female-specific pattern of DEGs conserved in both species.
167 That there is a component of the transcriptional response of microglia genes which is conserved
168 in both species and in both sexes, and that there is also a component of the response that shows
169 sex differences in both species are consistent with transcriptional reprograming in the dorsal horn
170 reported in the literature (*7, 8*) . Thus, we conclude that our approach of combining
171 transcriptional profiles of sex and species together has face validity. By combining sex and
172 species data we expected to have greater power than previous studies, and indeed we found
173 changes in expression of genes for neuronal processes specifically in females, a finding not
174 revealed by previous analyses.

175

176 **Defining a gene regulatory interactome network after peripheral nerve injury**

177 We investigated whether there may be patterns in the repertoire of transcription factors
178 regulating expression of the genes differentially expressed in the dorsal horn following nerve
179 injury. To this end we used the ChEA3 database (*15*) which integrated six databases containing
180 experimentally defined transcription factor binding sites identified by chromatin-immune
181 precipitation sequencing. We interrogated the ChEA3 database with the 93 conserved DEGs
182 identified above. With the set of DEGs common across sex and species and with a cutoff of
183 $p<0.01$ we identified 37 transcription factors (Fig. 4A, fig. S6 and Table.S4). Unsupervised
184 hierarchical cluster analysis revealed 2 major clusters within the 93 conserved DEGs (Fig. 4B).
185 Two of the transcription factors expressed in microglia that had not been previously linked to

186 pain hypersensitivity are Lymphoblastic Leukemia Associated Hematopoiesis Regulator 1
187 (LYL1) and IKAROS Family Zinc Finger 1 (IKZF1). These transcription factors regulate 72%
188 and 42%, respectively, of the common DEGs (Fig. 4C). We verified by PCR that expression of
189 Ikzf1 was increased after SNI, in a new cohort of male and female mice and rat (fig. S4A).

190 We next analyzed transcription factor regulatory network in males and females
191 separately. To investigate which transcription factors are contributing to the differential gene
192 expression, we used the common DEGs in male of both species (n=144), and likewise in
193 females, (n=114) (Fig. 4D). We found male and female rodents utilize transcription factors with
194 different priority (Fig. 4E). For the lower ranked transcription factors there was increasing
195 divergence in the rank order between males and females. We identified two male-specific
196 (CEBPB, ELF4) and two female-specific (ARID3A, MEF2B) transcription factors. These
197 transcription factors are reported to be expressed principally in microglia cells and in T cells,
198 respectively (*16, 17*) (Fig. 4D, Table. S4).

199

200 **Targeting the sex- and species-conserved neuropathic pain interactome.**

201 As the DEGs and transcription factor networks in males and females were largely similar
202 in both species, we wondered whether we could use the common DEGs to identify drugs that
203 might reduce pain hypersensitivity in both sexes. From the proteins encoded by these DEGs we
204 constructed a Protein-Protein Interaction (PPI) network using STRING (https://string-db.org)
205 (*18*) This network was constructed with interaction scores greater than 0.9 and visualized in
206 Cytoscape (*19*) (Fig. 5A, table S5). The resultant PPI network contained 38 nodes and 67 edges
207 (interactions) which is significantly greater than predicted by a set of 93 proteins drawn
208 randomly from the genome (PPI enrichment p-value $< 1.0e{-}16$). To identify the most influential

209 nodes within the PPI network we calculated the Integrated Value of Influence (IVI) (*20*) for each
210 node (table S6).

211 Separately, we interrogated the database of FDA-approved drugs – the Drug-Gene
212 Interaction (DGIdb v4.1.0) (*21*) – with the list of 93 conserved DEGs. In the DGIdb we
213 identified 186 drugs that affect one or more of the common genes (table S7). In order to find top
214 FDA approved drugs that can target multiple influential nodes we calculated the Drug impact for
215 each drug from the equation below (table S8).

216 $$Drug\,impact = \frac{\sum_{i=1}^{n} IVI \times n}{t}$$

217 where *n* is representative of number of genes that are impacted by each drug and *t* is total number
218 of nodes in the network. The five top-ranked were: 1- Fostamatinib, 2-Imatinib, 3-
219 Bevacizumab, Daclizumab, Palivizumab, 4- Ibrutinib and 5- Etanercept. (Table 2).

220 From this approach we predicted that drugs affecting the most influential nodes in the PPI
221 network may inhibit pain hypersensitivity in both sexes. We tested this prediction for the top-
222 ranked drug, fostamatinib. Fostamatinib is a pro-drug which yields the active molecule R406 by
223 metabolism in the liver (*22*). We tested the effect of R406 in males and females seven days after
224 SNI (Fig. 5C). Given that we implicated R406 from analyzing transcriptomes from the dorsal
225 horn, we administered this drug intrathecally. We found that R406 significantly reversed SNI-
226 induced mechanical hypersensitivity starting within 15 (p= 0.0016) and 30 mins (p= 0.0430) of
227 the i.t. injection (Fig. 5D) with the effect in males indistinguishable from that in females (Fig.
228 5D and fig. S7). These findings are evidence confirming our prediction from the analysis of the
229 PPI network and the DGIdb that a drug not previously associated with pain may reverse chronic
230 pain hypersensitivity.

231 **DISCUSSION**

232 Here, we generated a species-conserved, sex-conserved SNI-induced pain interactome network
233 and, with an unsupervised approach, predicted safe therapies that might have the most impact in
234 the interactome and thus might suppress pain hypersensitivity. We found that intrathecally
235 administering R406, the active metabolite of the top-ranked FDA-approved drug fostamatinib,
236 reversed mechanical hypersensitivity providing proof-of-concept to our approach. R406/
237 fostamatinib, which is clinically used to treat idiopathic thrombocytopenia purpura, was designed
238 to suppress the kinase activity of spleen tyrosine kinase (Syk) (*23, 24*) making this kinase the
239 most likely molecular target for the pain-reducing activity of this drug. We observed that Syk
240 mRNA is substantially elevated in the ipsilateral dorsal horn by SNI providing a biologically
241 plausible explanation for the effectiveness of R406. Moreover, the pain interactome includes
242 upstream activators of Syk, Trem2 and CCR5, and downstream effectors in Syk signaling, VAV
243 and PI3 kinase (Fig. 5D). R406 has been found to suppress the activity of a number of kinases
244 and receptors (*25-28*) and thus a combined effect on multiple sites in the interactome network,
245 in addition to its inhibition of Syk, may contribute to the analgesic action we discovered.

246 Syk is known to be expressed strongly in immune cells particularly macrophages,
247 microglia, dendritic cells and B lymphocytes (*25*). The reversal of mechanical hypersensitivity
248 by R406 in females as well as males may seem to suggest that the cell type affected by this drug
249 is not microglia as interventions that suppress or ablate microglia differentially reverse pain
250 hypersensitivity in males but not in females (*29*). This would be the case if R406 acts to
251 suppress a pain-driving signal from microglia. But if R406 acts to induce microglia, or a subset
252 thereof, to produce a pain-reducing signal then microglia could be the cell type in which R406
253 acts. Recently, a subtype of microglia, expressing cd11c, was reported to actively reverse

254 hypersensitivity (*30*) in both sexes raising the possibility that R406 may act on this microglia
255 subtype which strongly expresses Syk and for which the molecular signature gene, Itgax, is in
256 the SNI-induced pain interactome (Fig. 5D). Alternatively, or in addition, meningeal
257 macrophages, which are known to express Syk, have been implicated in controlling SNI-induced
258 pain hypersensitivity (*16*) . While it appears that the most likely role for Syk, and hence the
259 effect of R406, is in immune cells in the spinal cord, we cannot rule out an effect in neurons as a
260 small proportion of three subtypes of excitatory neurons in the dorsal horn are reported to
261 express Syk mRNA *de novo* after SNI (*16*) An effect of R406, directly or indirectly, on the
262 cellular, neuronal processes of underlying SNI-induced pain hypersensitivity is consistent with
263 the reported degeneracy of upstream immune cell signaling and the ultimate sex- and species-
264 commonality of the principal pathological neuronal alterations, i.e. downregulation of the
265 potassium-chloride cotransporter KCC2 and enhanced function GluN2B-containing NMDA
266 receptors (*31*) .

267 From the 93 sex-conserved and species-conserved genes, the role of the proteins encoded
268 by 17 of these genes in neuropathic pain has not been investigated to date (table S9). Based on
269 gene ontology analysis, out of this 17 DEGs, Hck, Blnk, Sla, Lcp2 are involved in
270 transmembrane receptor protein tyrosine kinase signaling pathway (table S10). the interaction of
271 these genes and spleen tyrosine kinase needs to be further investigated.

272 In addition to defining the sex- and species-common genes, we explored the expression
273 of genes for transcription factors that can regulate may regulate expression of these genes. We
274 found that eight of the top 10 transcription factors have been linked to pain. Specifically, IRF5,
275 the top-ranked transcription factor, is well-known to be markedly upregulated after peripheral
276 nerve injury, and reducing expression of IRF5 prevents development of pain hypersensitivity in

277 mice (*32, 33*). Two of the transcription factors we identified, Lyl1 and Ikzf1, have not been
278 previously implicated in chronic pain hypersensitivity. Lyl1 is a basic helix-loop-helix (bHLH)
279 type of transcription factor known to play a role on cell proliferation and differentiation and have
280 a role on macrophages and microglia development (*34, 35*). IKZF1 is a type of lymphoid-
281 restricted zinc finger transcription factor is known to regulate immune cells (*36*). It has been
282 shown that Syk plays a crucial role for IKZF1 activation (*37*), therefore, R406 have a potential to
283 disrupt IKZF1 nuclear localization and result in suppressing of IKZF1 targets.

284 The focus of the present paper on sex-conserved and species-conserved genes may seem
285 contrary to a goal of considering sex as a biological variable in chronic pain (*38*). This focus
286 was revealed by the results of our experimental and analytical design, and was only possible by
287 examining both sexes, and both species, of rodents. It was only through testing and analyzing
288 animals of both sexes that we were able to define those changes that are sex-different or sex-
289 conserved without biasedly assuming that changes elucidated by studying only one sex, by far
290 males, will generalize to the other sex. We did find sex differences in the transcriptional
291 reprograming of the dorsal horn that were conserved in both rats and mice. Surprisingly, given
292 past studies, we found evidence for differential cell type transcriptional changes induced by PNI
293 linked to neurons. Specifically, the genes upregulated in female mice and rats were, to a first
294 approximation, preferentially expressed in dorsal horn neurons. Exploring the role of the genes
295 and gene networks discovered by this analysis therefore opens up the possibility of investigating
296 the causal, i.e. necessary and sufficient, roles of proteins encoded by the genes we have
297 identified as sex-specific. From our analysis it is apparent that transcriptional reprograming in
298 the spinal dorsal horn in response to SNI has both sex-different and sex-conversed components.

299 In conclusion, we demonstrated that there is transcriptional reprograming in response to
300 peripheral nerve injury that is conserved across sex and species. From deconvolving the species-
301 conserved, sex-conserved pain interactome with the DGIdb database we created a ranking of
302 FDA-approved drugs that we hypothesized may impact the pain interactome network. Given
303 that the top hit, R406, pharmacologically inhibits Syk from humans and rodents (*23*), our
304 discovery that this drug reverses SNI-induced mechanical hypersensitivity predicts that
305 fostamatinib may reduce neuropathic pain humans, a prediction that is testable. We anticipate
306 that our findings will provide a rational basis for speeding testing of potential analgesic agents,
307 such as fostamatinib and others that impact the nerve injury-induced pain interactome, and
308 therefore accelerate the pace of bringing new therapeutic options to those suffering with
309 neuropathic pain.

310

311 **MATERIALS AND METHODS**

312 **Study Design**

313 Male and female C57BL/6J mice (n=6 per sex per condition aged 6-8 weeks) and Sprague
314 Dawley rats (n=4 per sex per condition 7-8 weeks age) were purchased from The Jackson and
315 Charles River laboratories at least two weeks before surgeries. All animals were housed in a
316 temperature-controlled environment with ad libitum access to food and water and maintained on
317 a 12:12-h light/dark cycle. In all experiments, animals were assigned to experimental groups
318 using randomization. Experimenters were blinded to drugs and sex where possible; blinding to
319 sex was ¬not possible in behavioural experiments. All experiments were performed with the
320 approval of the Hospital for Sick Children's Animal Care Committee and in compliance with the
321 Canadian Council on Animal Care guidelines.

322 **Peripheral nerve injury**

323 Neuropathic pain was induced in rodents using the spared nerve injury (SNI) model (Decosterd
324 & Woolf, 2000). Briefly, animals were anesthetized with 2.5% isoflurane/oxygen under sterile
325 conditions. An incision was made on the biceps femoris muscle's left thigh and blunt dissection
326 to expose the sciatic nerve. As a control, sham surgery was performed with all steps except
327 sciatic nerve manipulation. The common peroneal and tibial nerves were tightly ligated and
328 transected in the SNI model but left the sural nerve intact. The muscle and skin incisions were
329 closed using 6-0 vicryl sutures in both groups.

330

331 **Tissue collection, library preparation and RNA sequencing**

332 Animals were euthanized, and the L4-L5 lumbar dorsal horn of the spinal cord was harvested
333 postoperative day 7 to study transcriptional changes. RNA was extracted from the tissue and
334 preserved in RNALater (Invitrogen), and the library was prepared and sequenced using Illumina
335 HiSeq 4000 by TCAG at The Hospital for Sick Children. The filtered reads are aligned to a
336 reference genome using STAR (*39*). The genome used in this analysis was Mus musculus
337 (GRCm38-mm10.0) and Rattus Norvegicus assembly (Rnor_6.0) after quality control, we
338 calculated log2(CPM) (counts-per-million reads), and ran principal component analysis The
339 differential gene expression analysis is done using DESeq2 (*40*) and edgeR (*41*) Bioconductor
340 packages. Genes with adjusted p-Value <0.01 and fold changes greater than |0.5| were defined
341 as differentially expressed genes (DEGs). In this study total of 24 samples from mice and 32
342 samples from rats were analyzed. We used three control groups (Sham_ipsi, Sham_contra and
343 SNI_ipsi) as a reference to find differential expressed genes.

344 **Exploratory Analysis**

345 Unsupervised hierarchal clustering was done by Euclidean method, number of optimal clusters
346 were calculated using Elbow method in R. Enrichment analysis was performed on the DEG list
347 using the Functional Annotation Tool in the DAVID website (https://david.ncifcrf.gov/) The
348 protein-protein interaction (PPI) network of the proteins encoded by the DEGs was investigated
349 using STRING v11.0 (*18*) to visualize protein-protein interaction. We used Cytoscape (*19*)
350 Interactions with a score larger than 0.9 (highest confidence) were selected to construct PPI
351 networks. Single edges not connected to the main network were removed. Transcription Factor
352 enrichment analysis was performed using ChEA3, a comprehensive curated library of
353 transcription factor targets that combines results from ENCODE and literature-based ChIP-seq
354 experiments (*15*). Deconvolution of bulk RNA seq into immune cell types was evaluated using
355 scMappR (*13*). The Drug Gene Interaction Database (DGIdb v4.1.0, www.dgidb.org) has been
356 used to predict potential therapy for pain interactome (*21*) The integrated value of influence (IVI)
357 was calculated by Influential R package (*20*). The impact of the drugs was calculated based on
358 equation below:

$$Drug\ impact = \frac{Sum\ IVI_{genes} \times Number\ of\ genes}{Total\ number\ of\ nodes}$$

360

361

362 **Quantitative real-time reverse transcription-polymerase chain reaction**

363 RNA was isolated by digesting L4:L5 spinal cord tissues in TRIZOL (Life Technologies) and
364 cDNA synthesized using the SuperScript VILO cDNA kit (Life Technologies). qPCR was
365 performed for 40 cycles (95 °C for 1 s, 60 °C for 20 s). Levels of the target genes were

366 normalized against the average of four housekeeping genes (Hprt1 in mice and Eef2 in rats) and
367 interpreted using the ΔΔCt method.
368
369 **Drug**
370 R406 were purchased from Axon Medchem LLC (R406-1674). It was dissolved in DMSO, and
371 corn oil Doses were determined in pilot experiments. Seven days post-SNI, rats were removed
372 from their cubicles, lightly anesthetized using isoflurane/oxygen, and given intrathecal injections
373 of R406 (1mg), in a volume of 20ul by 30-gauge needle.
374
375 **Behavioural test**
376 Animals were randomized in experimental groups and behavioural experimenter was unaware of
377 the treatment or design of the study. The mechanical withdrawal threshold of animals was tested
378 on the ipsilateral paw using calibrated von Frey filaments of increasing logarithmic nominal
379 force values. Animals were placed in custom-made Plexiglas cubicles on a perforated metal
380 floor and were permitted to habituate for at least one hour before testing. Filaments were applied
381 to the perpendicular plantar surface of the hind paw for one second. A positive response was
382 recorded if there was a quick withdrawal, licking, or shaking of the paw by the animal. Each
383 filament was tested five times with increasing force filaments (1-26g) used until a filament in
384 which three out of five applications resulted in a paw withdrawal or when the maximal force
385 filament was reached. This filament force is called the mechanical withdrawal threshold. The
386 behavioural data is normalized as either percentage of baseline or presented as percent
387 hypersensitivity.

388

389 **Statistical analysis**

390 RNA-seq datasets were analyzed in R studio. For behavioral and Realtime PCR data, datasets
391 were tested for normality using the Shapiro-Wilk test. qPCR data analyzed with the "pcr" R
392 package, and behavioral data were analyzed by GraphPad Prism 9.3.1. One-way analysis of
393 variance (ANOVA) or Kruskal-Wallis test was performed when comparisons were made across
394 more than two groups. Two-way ANOVA (Bonferroni's multiple) was used to test differences
395 between two or more groups. T-test was performed to test differences between two groups.
396 Statistical significance refers to *$p< 0.05$, ** $p< 0.01$, *** $p< 0.001$ Data are presented as mean
397 ± SEM.

398

References

1. J. Dahlhamer, J. Lucas, C. Zelaya, R. Nahin, S. Mackey, L. DeBar, R. Kerns, M. Von Korff, L. Porter, C. Helmick, Prevalence of Chronic Pain and High-Impact Chronic Pain Among Adults - United States, 2016. *MMWR. Morbidity and mortality weekly report* **67**, 1001-1006 (2018).
2. A. S. C. Rice, B. H. Smith, F. M. Blyth, Pain and the global burden of disease. *Pain* **157**, 791-796 (2016).
3. S. N. Raja, D. B. Carr, M. Cohen, N. B. Finnerup, H. Flor, S. Gibson, F. J. Keefe, J. S. Mogil, M. Ringkamp, K. A. Sluka, X. J. Song, B. Stevens, M. D. Sullivan, P. R. Tutelman, T. Ushida, K. Vader, The revised International Association for the Study of Pain definition of pain: concepts, challenges, and compromises. *Pain* **161**, 1976-1982 (2020).
4. M. van Velzen, A. Dahan, M. Niesters, Neuropathic Pain: Challenges and Opportunities. *Frontiers in pain research (Lausanne, Switzerland)* **1**, 1-1 (2020).
5. R. P. Yezierski, P. Hansson, Inflammatory and Neuropathic Pain From Bench to Bedside: What Went Wrong? *J Pain* **19**, 571-588 (2018).
6. M. Costigan, J. Scholz, C. J. Woolf, Neuropathic pain: a maladaptive response of the nervous system to damage. *Annual review of neuroscience* **32**, 1-32 (2009).
7. M. Parisien, A. Samoshkin, S. N. Tansley, M. H. Piltonen, L. J. Martin, N. El-Hachem, C. Dagostino, M. Allegri, J. S. Mogil, A. Khoutorsky, L. Diatchenko, Genetic pathway analysis reveals a major role for extracellular matrix organization in inflammatory and neuropathic pain. *Pain* **160**, 932-944 (2019).
8. F. H. G. Ahlström, K. Mätlik, H. Viisanen, K. J. Blomqvist, X. Liu, T. O. Lilius, Y. Sidorova, E. A. Kalso, P. V. Rauhala, Spared Nerve Injury Causes Sexually Dimorphic Mechanical Allodynia and Differential Gene Expression in Spinal Cords and Dorsal Root Ganglia in Rats. *Molecular neurobiology* **58**, 5396-5419 (2021).
9. S. Tansley, S. Uttam, A. Ureña Guzmán, M. Yaqubi, A. Pacis, M. Parisien, H. Deamond, C. Wong, O. Rabau, N. Brown, L. Haglund, J. Ouellet, C. Santaguida, A. Ribeiro-da-Silva, S. Tahmasebi, M. Prager-Khoutorsky, J. Ragoussis, J. Zhang, M. W. Salter, L. Diatchenko, L. M. Healy, J. S. Mogil, A. Khoutorsky, Single-cell RNA sequencing reveals time- and sex-specific responses of mouse spinal cord microglia to peripheral nerve injury and links ApoE to chronic pain. *Nature communications* **13**, 843 (2022).
10. N. T. Fiore, Z. Yin, D. Guneykaya, C. D. Gauthier, J. P. Hayes, A. D'Hary, O. Butovsky, G. Moalem-Taylor, Sex-specific transcriptome of spinal microglia in neuropathic pain due to peripheral nerve injury. *Glia* **70**, 675-696 (2022).
11. I. Decosterd, C. J. Woolf, Spared nerve injury: an animal model of persistent peripheral neuropathic pain. *Pain* **87**, 149-158 (2000).
12. T. Yu, X. Zhang, H. Shi, J. Tian, L. Sun, X. Hu, W. Cui, D. Du, P2Y12 regulates microglia activation and excitatory synaptic transmission in spinal lamina II neurons during neuropathic pain in rodents. *Cell death & disease* **10**, 165 (2019).
13. D. J. Sokolowski, M. Faykoo-Martinez, L. Erdman, H. Hou, C. Chan, H. Zhu, M. M. Holmes, A. Goldenberg, M. D. Wilson, Single-cell mapper (scMappR): using scRNA-seq to infer the cell-type specificities of differentially expressed genes. *NAR genomics and bioinformatics* **3**, lqab011 (2021).

14. O. Franzén, L. M. Gan, J. L. M. Björkegren, PanglaoDB: a web server for exploration of mouse and human single-cell RNA sequencing data. *Database : the journal of biological databases and curation* **2019**, (2019).
15. A. B. Keenan, D. Torre, A. Lachmann, A. K. Leong, M. L. Wojciechowicz, V. Utti, K. M. Jagodnik, E. Kropiwnicki, Z. Wang, A. Ma'ayan, ChEA3: transcription factor enrichment analysis by orthogonal omics integration. *Nucleic Acids Res* **47**, W212-W224 (2019).
16. J. K. Niehaus, B. Taylor-Blake, L. Loo, J. M. Simon, M. J. Zylka, Spinal macrophages resolve nociceptive hypersensitivity after peripheral injury. *Neuron* **109**, 1274-1282.e1276 (2021).
17. M. Uhlen, M. J. Karlsson, W. Zhong, A. Tebani, C. Pou, J. Mikes, T. Lakshmikanth, B. Forsström, F. Edfors, J. Odeberg, A. Mardinoglu, C. Zhang, K. von Feilitzen, J. Mulder, E. Sjöstedt, A. Hober, P. Oksvold, M. Zwahlen, F. Ponten, C. Lindskog, Å. Sivertsson, L. Fagerberg, P. Brodin, A genome-wide transcriptomic analysis of protein-coding genes in human blood cells. *Science (New York, N.Y.)* **366**, (2019).
18. D. Szklarczyk, A. L. Gable, D. Lyon, A. Junge, S. Wyder, J. Huerta-Cepas, M. Simonovic, N. T. Doncheva, J. H. Morris, P. Bork, L. J. Jensen, C. V. Mering, STRING v11: protein-protein association networks with increased coverage, supporting functional discovery in genome-wide experimental datasets. *Nucleic Acids Res* **47**, D607-d613 (2019).
19. P. Shannon, A. Markiel, O. Ozier, N. S. Baliga, J. T. Wang, D. Ramage, N. Amin, B. Schwikowski, T. Ideker, Cytoscape: a software environment for integrated models of biomolecular interaction networks. *Genome research* **13**, 2498-2504 (2003).
20. A. Salavaty, M. Ramialison, P. D. Currie, Integrated Value of Influence: An Integrative Method for the Identification of the Most Influential Nodes within Networks. *Patterns (New York, N.Y.)* **1**, 100052 (2020).
21. S. L. Freshour, S. Kiwala, K. C. Cotto, A. C. Coffman, J. F. McMichael, J. J. Song, M. Griffith, Obi L. Griffith, A. H. Wagner, Integration of the Drug–Gene Interaction Database (DGIdb 4.0) with open crowdsource efforts. *Nucleic Acids Research* **49**, D1144-D1151 (2020).
22. D. J. Sweeny, W. Li, J. Clough, S. Bhamidipati, R. Singh, G. Park, M. Baluom, E. Grossbard, D. T. Lau, Metabolism of fostamatinib, the oral methylene phosphate prodrug of the spleen tyrosine kinase inhibitor R406 in humans: contribution of hepatic and gut bacterial processes to the overall biotransformation. *Drug metabolism and disposition: the biological fate of chemicals* **38**, 1166-1176 (2010).
23. A. Podolanczuk, A. H. Lazarus, A. R. Crow, E. Grossbard, J. B. Bussel, Of mice and men: an open-label pilot study for treatment of immune thrombocytopenic purpura by an inhibitor of Syk. *Blood* **113**, 3154-3160 (2009).
24. J. Paik, Fostamatinib: A Review in Chronic Immune Thrombocytopenia. *Drugs* **81**, 935-943 (2021).
25. A. Mócsai, J. Ruland, V. L. J. Tybulewicz, The SYK tyrosine kinase: a crucial player in diverse biological functions. *Nat Rev Immunol* **10**, 387-402 (2010).
26. L. Wang, D. Aschenbrenner, Z. Zeng, X. Cao, D. Mayr, M. Mehta, M. Capitani, N. Warner, J. Pan, L. Wang, Q. Li, T. Zuo, S. Cohen-Kedar, J. Lu, R. C. Ardy, D. J. Mulder, D. Dissanayake, K. Peng, Z. Huang, X. Li, Y. Wang, X. Wang, S. Li, S. Bullers, A. N. Gammage, K. Warnatz, A. I. Schiefer, G. Krivan, V. Goda, W. H. A. Kahr, M. Lemaire,

C. Y. Lu, I. Siddiqui, M. G. Surette, D. Kotlarz, K. R. Engelhardt, H. R. Griffin, R. Rottapel, H. Decaluwe, R. M. Laxer, M. Proietti, S. Hambleton, S. Elcombe, C. H. Guo, B. Grimbacher, I. Dotan, S. C. Ng, S. A. Freeman, S. B. Snapper, C. Klein, K. Boztug, Y. Huang, D. Li, H. H. Uhlig, A. M. Muise, Gain-of-function variants in SYK cause immune dysregulation and systemic inflammation in humans and mice. *Nature genetics* **53**, 500-510 (2021).

27. S. Braselmann, V. Taylor, H. Zhao, S. Wang, C. Sylvain, M. Baluom, K. Qu, E. Herlaar, A. Lau, C. Young, B. R. Wong, S. Lovell, T. Sun, G. Park, A. Argade, S. Jurcevic, P. Pine, R. Singh, E. B. Grossbard, D. G. Payan, E. S. Masuda, R406, an orally available spleen tyrosine kinase inhibitor blocks fc receptor signaling and reduces immune complex-mediated inflammation. *The Journal of pharmacology and experimental therapeutics* **319**, 998-1008 (2006).
28. H.-J. Cho, E. J. Yang, J. T. Park, J.-R. Kim, E.-C. Kim, K.-J. Jung, S. C. Park, Y.-S. Lee, Identification of SYK inhibitor, R406 as a novel senolytic agent. *Aging (Albany NY)* **12**, 8221-8240 (2020).
29. R. E. Sorge, J. C. Mapplebeck, S. Rosen, S. Beggs, S. Taves, J. K. Alexander, L. J. Martin, J. S. Austin, S. G. Sotocinal, D. Chen, M. Yang, X. Q. Shi, H. Huang, N. J. Pillon, P. J. Bilan, Y. Tu, A. Klip, R. R. Ji, J. Zhang, M. W. Salter, J. S. Mogil, Different immune cells mediate mechanical pain hypersensitivity in male and female mice. *Nature neuroscience* **18**, 1081-1083 (2015).
30. K. Kohno, R. Shirasaka, K. Yoshihara, S. Mikuriya, K. Tanaka, K. Takanami, K. Inoue, H. Sakamoto, Y. Ohkawa, T. Masuda, M. Tsuda, A spinal microglia population involved in remitting and relapsing neuropathic pain. *Science (New York, N.Y.)* **376**, 86-90 (2022).
31. J. C. S. Mapplebeck, L. E. Lorenzo, K. Y. Lee, C. Gauthier, M. M. Muley, Y. De Koninck, S. A. Prescott, M. W. Salter, Chloride Dysregulation through Downregulation of KCC2 Mediates Neuropathic Pain in Both Sexes. *Cell reports* **28**, 590-596.e594 (2019).
32. T. Terashima, N. Ogawa, Y. Nakae, T. Sato, M. Katagi, J. Okano, H. Maegawa, H. Kojima, Gene Therapy for Neuropathic Pain through siRNA-IRF5 Gene Delivery with Homing Peptides to Microglia. *Molecular therapy. Nucleic acids* **11**, 203-215 (2018).
33. T. Masuda, S. Iwamoto, R. Yoshinaga, H. Tozaki-Saitoh, A. Nishiyama, T. W. Mak, T. Tamura, M. Tsuda, K. Inoue, Transcription factor IRF5 drives P2X4R+-reactive microglia gating neuropathic pain. *Nature communications* **5**, 3771 (2014).
34. S. Wang, D. Ren, B. Arkoun, A. L. Kaushik, G. Matherat, Y. Lécluse, D. Filipp, W. Vainchenker, H. Raslova, I. Plo, I. Godin, Lyl-1 regulates primitive macrophages and microglia development. *Communications biology* **4**, 1382 (2021).
35. S. San-Marina, Y. Han, F. Suarez Saiz, M. R. Trus, M. D. Minden, Lyl1 interacts with CREB1 and alters expression of CREB1 target genes. *Biochimica et biophysica acta* **1783**, 503-517 (2008).
36. A. S. Geimer Le Lay, A. Oravecz, J. Mastio, C. Jung, P. Marchal, C. Ebel, D. Dembélé, B. Jost, S. Le Gras, C. Thibault, T. Borggrefe, P. Kastner, S. Chan, The tumor suppressor Ikaros shapes the repertoire of notch target genes in T cells. *Science signaling* **7**, ra28 (2014).
37. F. M. Uckun, H. Ma, J. Zhang, Z. Ozer, S. Dovat, C. Mao, R. Ishkhanian, P. Goodman, S. Qazi, Serine phosphorylation by SYK is critical for nuclear localization and

transcription factor function of Ikaros. *Proceedings of the National Academy of Sciences of the United States of America* **109**, 18072-18077 (2012).

38. S. Ghazisaeidi, M. M. Muley, M. W. Salter, Neuropathic pain: Mechanisms, sex differences, and potential therapies for a global problem. *Annual Review of Pharmacology and Toxicology* **63**, (2023).

39. A. Dobin, C. A. Davis, F. Schlesinger, J. Drenkow, C. Zaleski, S. Jha, P. Batut, M. Chaisson, T. R. Gingeras, STAR: ultrafast universal RNA-seq aligner. *Bioinformatics (Oxford, England)* **29**, 15-21 (2013).

40. M. I. Love, W. Huber, S. Anders, Moderated estimation of fold change and dispersion for RNA-seq data with DESeq2. *Genome Biology* **15**, 550 (2014).

41. M. D. Robinson, D. J. McCarthy, G. K. Smyth, edgeR: a Bioconductor package for differential expression analysis of digital gene expression data. *Bioinformatics (Oxford, England)* **26**, 139-140 (2010).

549 **Acknowledgments:**

550 Authors would like to thank Dr. David Finn and Dr. Katherine Halievski, Vivian Wang, Sofia
551 Assi for technical assistance. This research was supported by a grant from CIHR (FDN-154336)
552 to MWS. MWS held the Northbridge Chair in Paediatric Research. SG was supported by
553 doctoral completion award and Massey College SAR, MMM was supported by a Pain Scientist
554 Award from the University of Toronto Centre for the Study of Pain, and by a Restracomp
555 postdoctoral fellowship from The Hospital for Sick Children Research Training Centre. Author
556 contributions: MWS, SG conceived the project; MWS, MB supervised the research; SG and YT
557 designed the experiments, MM, SG, YT designed in-vivo Fostamatinib experiment, SG, MM,
558 YT, MK collected data and executed in vivo experiments, SG, AKR performed bioinformatic
559 analysis, AS, AKR assisted with study design and interpretation of results. SG and MWS and
560 wrote the manuscript with input from all authors. Competing interests: Authors declare that they
561 have no competing interests. Data and materials availability: Data supporting the findings of this
562 study are available within the article and its Supplementary material files and from the
563 corresponding author upon reasonable request.

564

565 **Figures**

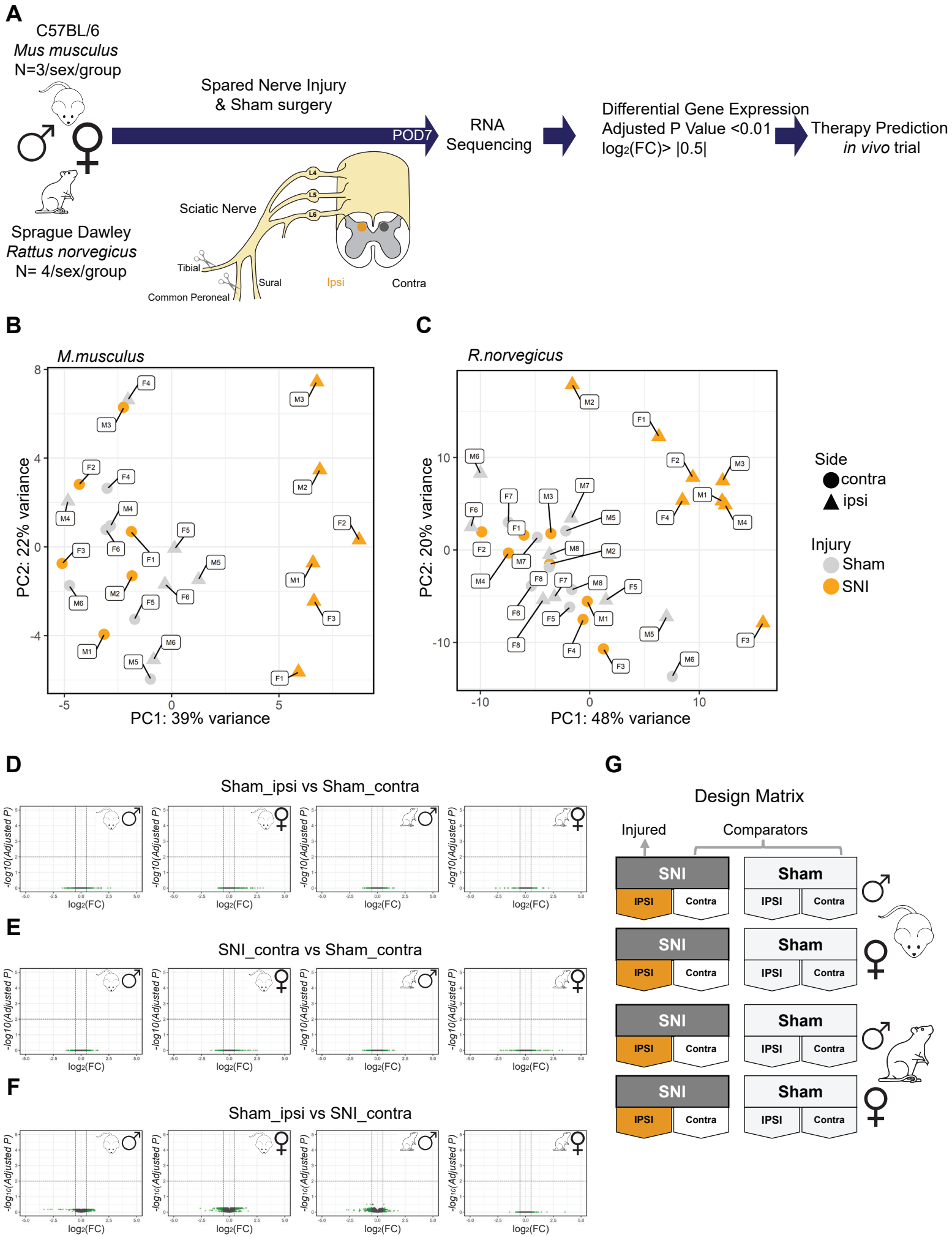
A
C57BL/6
Mus musculus
N=3/sex/group
Sprague Dawley
Rattus norvegicus
N= 4/sex/group
Spared Nerve Injury
& Sham surgery
POD7
RNA
Sequencing
Differential Gene Expression
Adjusted P Value <0.01
log2(FC)> |0.5|
Therapy Prediction
in vivo trial
Sciatic Nerve
L4
L5
L6
Tibial
Sural
Common Peroneal
Ipsi
Contra
B
M.musculus
PC2: 22% variance
PC1: 39% variance
C
R.norvegicus
PC2: 20% variance
PC1: 48% variance
Side
contra
ipsi
Injury
Sham
SNI
D
Sham_ipsi vs Sham_contra
E
SNI_contra vs Sham_contra
F
Sham_ipsi vs SNI_contra
-log10(Adjusted P)
log2(FC)
G
Design Matrix
Injured
Comparators
SNI
Sham
IPSI
Contra

Fig. 1. **Experimental Design and data overview.** (A) The experimental workflow is illustrated. (B-C) Scatter plot representing principal component analyses of the dimensions PC1 versus PC2 samples. (B) Principal component analysis in mice. (C) principal component analysis in rats. (D-F) Volcano plots showing pair-wise differential gene expression in male and female mice and rat between comparators. (D) Sham_ipsi vs Sham_contra. (E) SNI_contra vs Sham_contra. (F) Sham_ipsi vs SNI_contra. (G) Summary of all groups in design matrix.

556

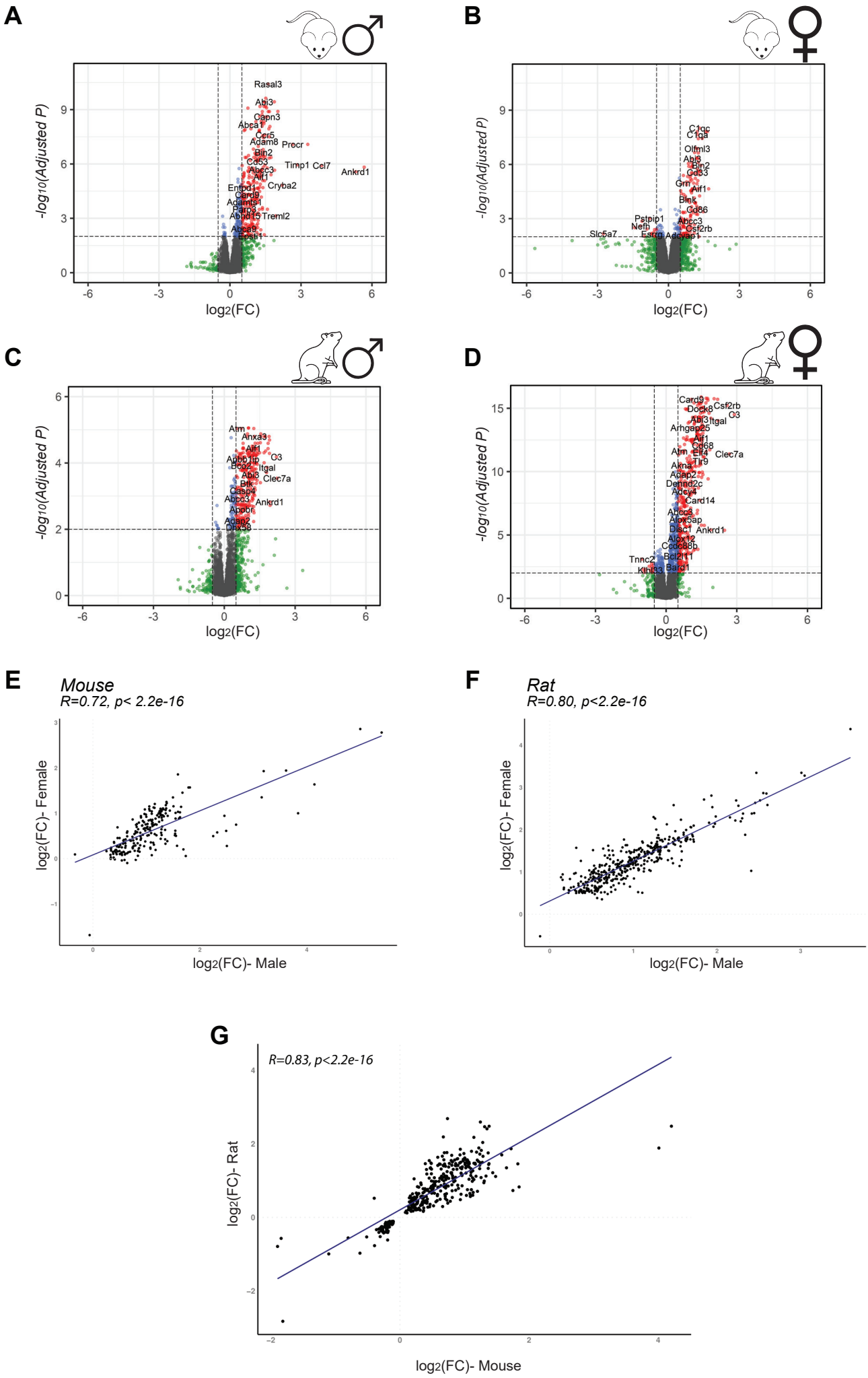
A
B
C
D
E
F
G
-log10(Adjusted P)
log2(FC)
Rasal3
Abi3
Capn3
Abca1
Ccr5
Adam8
Procr
Bin2
Cd53
Timp1
Ccl7
Ankrd1
Abcc3
Aif1
Cryba2
Entpd1
Card9
Adamts1
Ptpn3
Abhd12
Treml2
Abcc9
Epsin1
C1qc
C1qa
Olfml3
Bin2
Cd53
Grn
Aif1
Blnk
Cd86
Abcc3
Csf2rb
Pstpip1
Nefb
Esrrg
Adcyap1
Slc5a7
Atm
Anxa3
Aif1
Cd68
Apbb1ip
Bco2
Itgal
Abi3
Clec7a
Blk
Cd36
Abcc3
Ankrd1
Apobr
Adap2
Dlx3
Card9
Csf2rb
Dock8
O3
Abi3
Itgal
Arhgap25
Aif1
Cd68
Atm
Eif4
Clec7a
Akna
Tlr9
Adap2
Dennd2c
Adcy4
Card14
Abcc9
Alox5ap
Disc1
Ankrd1
Alox12
Ccl5
Tnnc2
Bcl2l11
Klhl33
Bard1
Mouse
R=0.72, p< 2.2e-16
log2(FC)- Female
log2(FC)- Male
Rat
R=0.80, p<2.2e-16
log2(FC)- Female
log2(FC)- Male
R=0.83, p<2.2e-16
log2(FC)- Rat
log2(FC)- Mouse

557 **Fig. 2. Transcriptome changes after SNI in male and female** rodents. (A-D) Volcano plots
558 were obtained by plotting the log2 fold change of SNI_ipsi against the negative Log10 of
559 the EdgeR adjusted p-value. Genes that changed 0.5 log2(FC) or more with a significance
560 of adj p-value <0.01 are shown red. Genes that were differentially expressed significantly
561 ($p < 0.01$) but changed less than 0.5 log2(FC) are highlighted in blue and black dots are
562 insignificant changes. (A) male mice, (B) female mice, (C) male rat and (D) female rat.
563 (E-G) Linear correlation of log2(FC) of SNI_ipsi vs comparators is demonstrated. Genes
564 that were differentially expressed in at least one dataset is considered. (E) Pearson
565 correlation in male and female mice. (F) Pearson correlation between male and female
566 rat. (G) and the Pearson correlation between mice and rat.

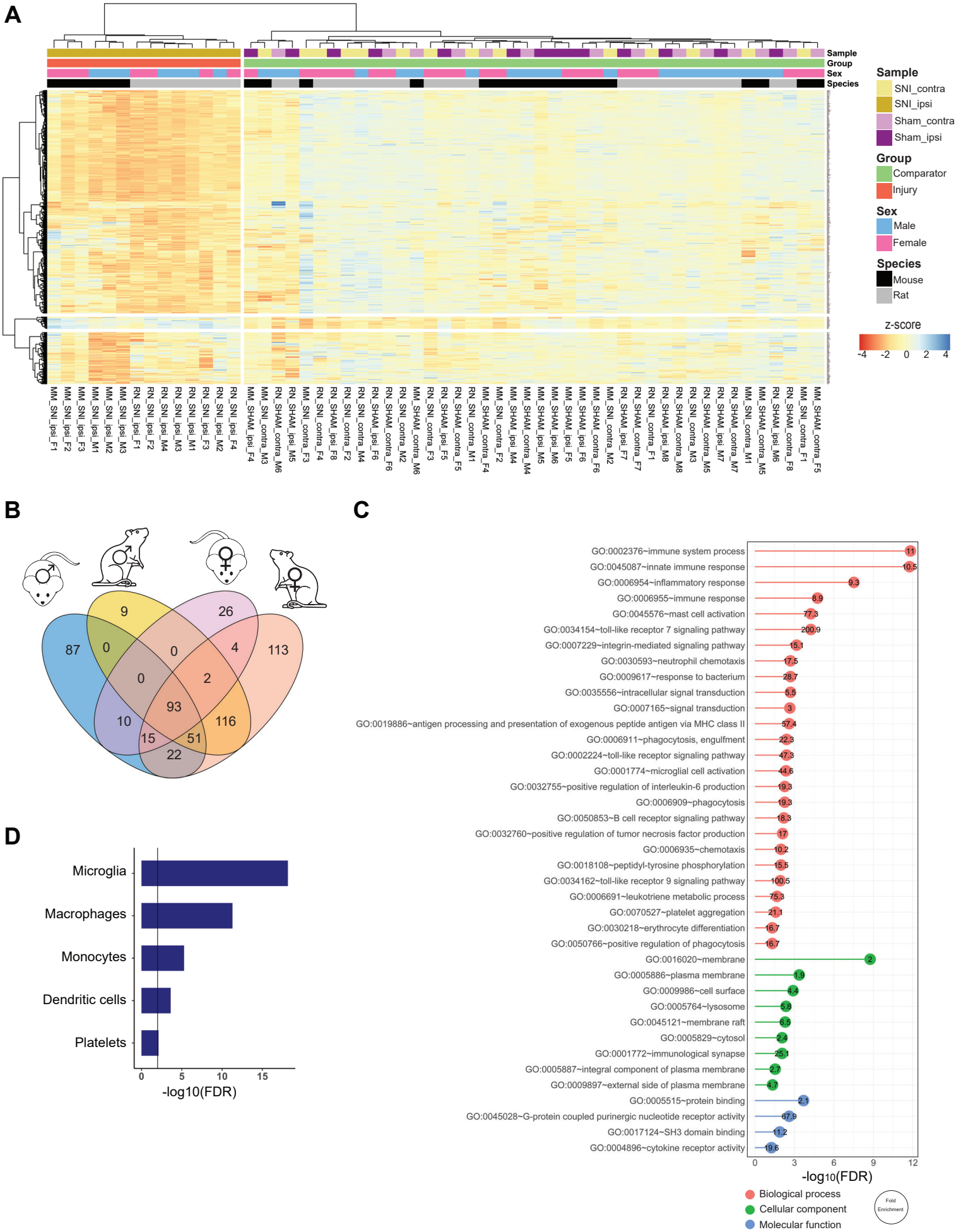
A
Sample
Group
Sex
Species
Sample
SNI_contra
SNI_ipsi
Sham_contra
Sham_ipsi
Group
Comparator
Injury
Sex
Male
Female
Species
Mouse
Rat
z-score
-4 -2 0 2 4
B
87
9
26
0
0
4
113
0
2
93
10
116
15
51
22
C
GO:0002376~immune system process
GO:0045087~innate immune response
GO:0006954~inflammatory response
GO:0006955~immune response
GO:0045576~mast cell activation
GO:0034154~toll-like receptor 7 signaling pathway
GO:0007229~integrin-mediated signaling pathway
GO:0030593~neutrophil chemotaxis
GO:0009617~response to bacterium
GO:0035556~intracellular signal transduction
GO:0007165~signal transduction
GO:0019886~antigen processing and presentation of exogenous peptide antigen via MHC class II
GO:0006911~phagocytosis, engulfment
GO:0002224~toll-like receptor signaling pathway
GO:0001774~microglial cell activation
GO:0032755~positive regulation of interleukin-6 production
GO:0006909~phagocytosis
GO:0050853~B cell receptor signaling pathway
GO:0032760~positive regulation of tumor necrosis factor production
GO:0006935~chemotaxis
GO:0018108~peptidyl-tyrosine phosphorylation
GO:0034162~toll-like receptor 9 signaling pathway
GO:0006691~leukotriene metabolic process
GO:0070527~platelet aggregation
GO:0030218~erythrocyte differentiation
GO:0050766~positive regulation of phagocytosis
GO:0016020~membrane
GO:0005886~plasma membrane
GO:0009986~cell surface
GO:0005764~lysosome
GO:0045121~membrane raft
GO:0005829~cytosol
GO:0001772~immunological synapse
GO:0005887~integral component of plasma membrane
GO:0009897~external side of plasma membrane
GO:0005515~protein binding
GO:0045028~G-protein coupled purinergic nucleotide receptor activity
GO:0017124~SH3 domain binding
GO:0004896~cytokine receptor activity
0 3 6 9 12
-log10(FDR)
Biological process
Cellular component
Molecular function
Fold Enrichment
D
Microglia
Macrophages
Monocytes
Dendritic cells
Platelets
0 5 10 15
-log10(FDR)

567 **Fig. 3. Peripheral nerve injury induces an immune response in rodents.** (A) Heatmap
568 showing the expression of the genes that were differentially expressed in at least one out
569 of four (male mice, female mice, male rat and female rat) datasets, z-scores were
570 calculated within species. (B) Venn diagram represents the number of differentially
571 expressed genes between datasets. (C) Gene ontology enrichment of 93 conserved genes,
572 biological processes are shown in pink, cellular components are shown in green and,
573 molecular function are shown in blue. (D) Bar chart represents deconvolution profile of
574 conserved genes obtained by scMappR package.
575

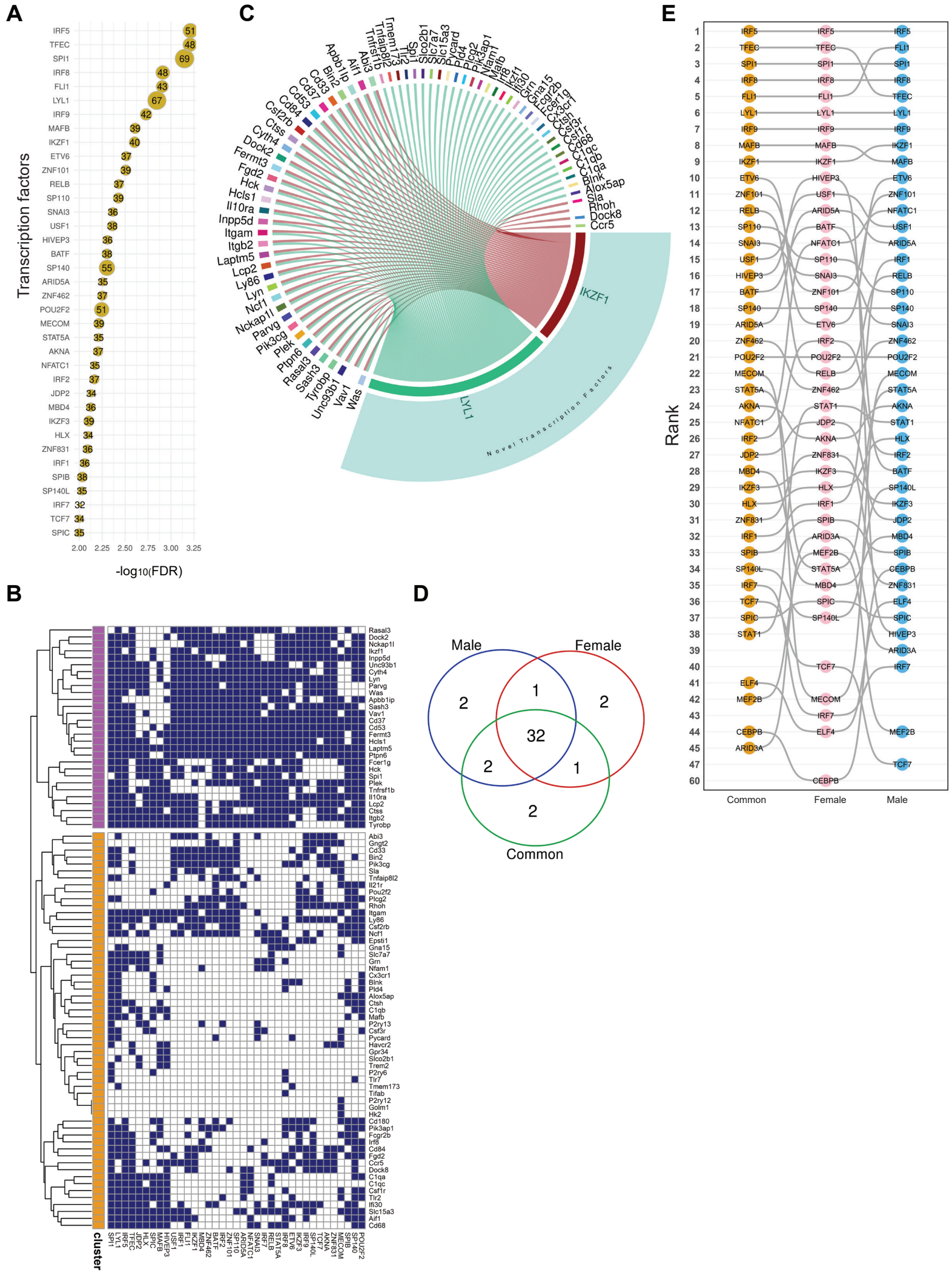
A
Transcription factors
-log10(FDR)
IRF5 51
TFEC 48
SPI1 69
IRF8 48
FLI1 43
LYL1 67
IRF9 42
MAFB 39
IKZF1 40
ETV6 37
ZNF101 39
RELB 37
SP110 39
SNAI3 36
USF1 38
HIVEP3 36
BATF 38
SP140 55
ARID5A 35
ZNF462 37
POU2F2 51
MECOM 39
STAT5A 35
AKNA 37
NFATC1 35
IRF2 37
JDP2 34
MBD4 36
IKZF3 39
HLX 34
ZNF831 36
IRF1 36
SPIB 38
SP140L 35
IRF7 32
TCF7 34
SPIC 35
2.00 2.25 2.50 2.75 3.00 3.25
B
cluster
C
IKZF1
LYL1
Novel Transcription Factors
E
Rank
Common
Female
Male
D
Male
Female
Common
2
1
2
32
2
1
2

576 **Fig 4. Gene regulation after peripheral nerve injury.** (A) bubble plot showing transcription
577 factors that can regulate conserved genes by ChEA3 database. (B) binary heatmap shows
578 transcription factors and their targets. (C) Circoplot showing the relation between two
579 novel transcription factors (LYL1 and IKZF1) and conserved genes. (D) Venn diagram
580 represents the number of transcription factors between male, female and combined male
581 and female datasets. (E) Bump chart visualizes the transcription factor ranking between
582 three datasets of male, female and common (E).

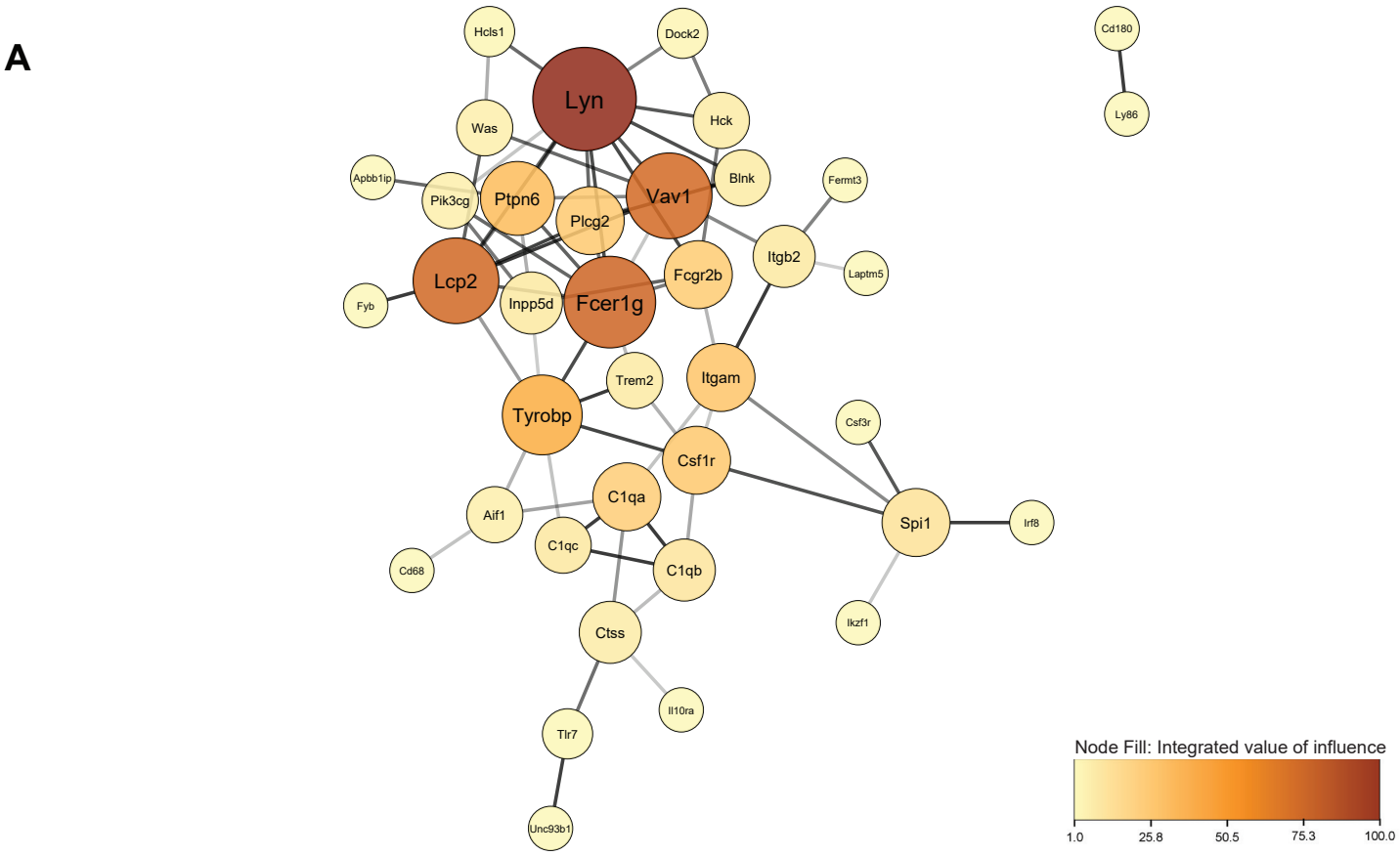
A
Hcls1
Dock2
Cd180
Lyn
Hck
Was
Ly86
Apbb1ip
Pik3cg
Ptpn6
Vav1
Blnk
Fermt3
Plcg2
Itgb2
Laptm5
Lcp2
Fcgr2b
Fyb
Inpp5d
Fcer1g
Trem2
Itgam
Tyrobp
Csf3r
Csf1r
C1qa
Aif1
Spi1
Irf8
C1qc
C1qb
Cd68
Ctss
Ikzf1
Il10ra
Tlr7
Unc93b1
Node Fill: Integrated value of influence
1.0
25.8
50.5
75.3
100.0


B
SNI
Day 0
Day 7
i.t. injection:
R406 (1mg)
or
Vehicle
♂ ♀
N=6/sex/group

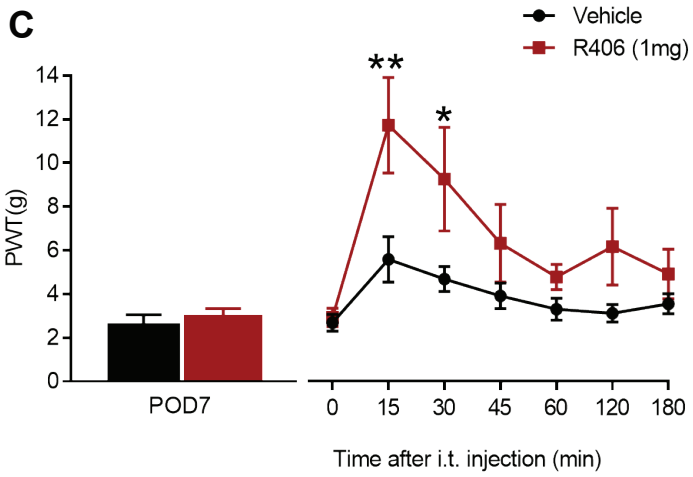
C
Vehicle
R406 (1mg)
**
*
PWT(g)
14
12
10
8
6
4
2
0
POD7
0
15
30
45
60
120
180
Time after i.t. injection (min)

583 **Fig 5. Targeting influential nodes inside conserved protein-protein interactome.**

584 (A) representing protein-protein interaction networks of conserved 93 DEGs retrieved
585 from STRING database. This interaction map was generated using the maximum
586 confidence (0.9). Color of the nodes is integrated the value of influence (IVI), Node size
587 is relative to the node degree. Nodes without any connection are hidden from the
588 network, edge thickness is based on evidence score. (B) Schematic diagram of
589 experimental design for R406 *in vivo* trial. (C) Paw withdrawal threshold from von Frey
590 filaments on the ipsilateral side 7 days after surgery in SNI animals, (N=6-
591 7/sex/treatment) and comparing SNI ipsilateral of R406 (1mg) and vehicle. Comparisons
592 were made by Bonferroni's multiple comparisons test *$p<0.05$, **$p<0.01$. Data are mean
593 ± SEM.

594 Table 1- List of primers for candidate targets

Species	Gene	Forward primer	Reverse Primer
Mouse	*Rasal3*	TCCGAGAAAATACCTTAGCCAC	GTCCACTTCACAGTCCTCAG
Rat	*Rasal3*	AGTGTCTGTACCAATGCGTC	AGACTGGCTCTTGGAAATGAG
Mouse	*Slco2b1*	CACTCCCTCACTTCATCTCAG	CATTGGACAGGGCAGAGG
Rat	*Slco2b1*	CACTCCCTCACTTCATCTCAG	TGGTTTCTGTGCGACTGG
Mouse	*Ikzf1*	CGCACAAATCCACATAACCTG	GGCTCATCCCCTTCATCTG
Rat	*Ikzf1*	TGGTTTCTGTGCGACTGG	ATCCTAACTTCTGCCGTAAGC
Mouse	*P2ry12*	TAACCATTGACCGATACCTGAAGA	TTCGCACCCAAAAGATTGC
Rat	*P2ry12*	CAGGTTCTCTTCCCATTGCT	CAGCAATGATGATGAAAACC
Mouse	*Hprt1*	CCCCAAAATGGTTAAGGTTGC	AACAAAGTCTGGCCTGTATCC
Rat	*Eef2*	ACTGACACTCGCAAGGATG	GGAGAGTCGATGAGGTTGATG

595

596 Table 2- list of top FDA approved drugs

Rank	Top FDA Drug	Class	Targets in the network	Drug Impact
1	Fostamatinib	Tyrosine kinase inhibitor	PIK3CG, HCK, LYN, CSF1R, CTSS, FCGR2B	26.25
2	Imatinib	Tyrosine kinase inhibitor	PIK3CG, HCK, LYN, CSF1R, IKZF1	18.14
3	Bevacizumab	anti-vascular endothelial growth factor antibody	C1QA, C1QB, C1QC, FCGR2B	6.63
	Palivizumab	Anti-respiratory syncytial virus F protein antibody	C1QA, C1QB, C1QC, FCGR2B	
	Daclizumab	CD25 antibody	C1QA, C1QB, C1QC, FCGR2B	
4	Ibrutinib	Tyrosine kinase inhibitor	LYN, PLCG2	6.53
5	Etanercept	Tumor necrosis factor alpha receptor inhibitor	TNFRSF1B, C1QA, FCGR2B, CD84,	4.67

597

598 **Supplementary Materials:**

599 **Supplementary Figures**

600 fig. S1- Principal components of mouse and rat datasets.

601 fig. S2- Pairwise comparison of SNI_ipsi vs each of the comparators.

602 fig. S3- Overview of differential gene expression in mice and rat datasets.

603 fig. S4- RNA-seq validation.

604 fig. S5- Gene ontology analysis and cell type profile for DEGs exclusive to sex or species.

605 fig. S6- Gene regulation of conserved genes.

606 fig. S7- R406 efficacy in male and female rats

607 **Supplementary Tables:**

608 table S1. Differentially expressed genes between four datasets.

609 table S2. Gene Ontology results for conserved genes.

610 table S3. Single cell deconvolution of conserved genes

611 table S4- List of transcription factors regulating conserved genes within sex and species

612 table S5- Protein-Protein interaction network

613 table S6- Integrated Value of Influence for conserved nodes

614 table S7. Drug interaction with conserved genes

615 table S8- Drug impact calculation on network

616 table S9- List of novel targets

617 table S10- Gene ontology analysis for 17 novel genes

618

619

620 **Abbreviations:**

621 CNS: Central Nervous System

622 SNI: Spared Nerve Injury

623 Ipsi: Ipsilateral

624 Contra: Contralateral

625 DEG(s): Differentially Expressed Gene(s)

626 PC: Principal Component

627 i.t. : Intrathecal

628 IVI: Integrated Value of Influence

629 PPI: Protein-Protein-Interaction

630 DGIdb: Drug Gene Interaction Database

631 SYK: Spleen tyrosine Kinase

Supplementary Materials

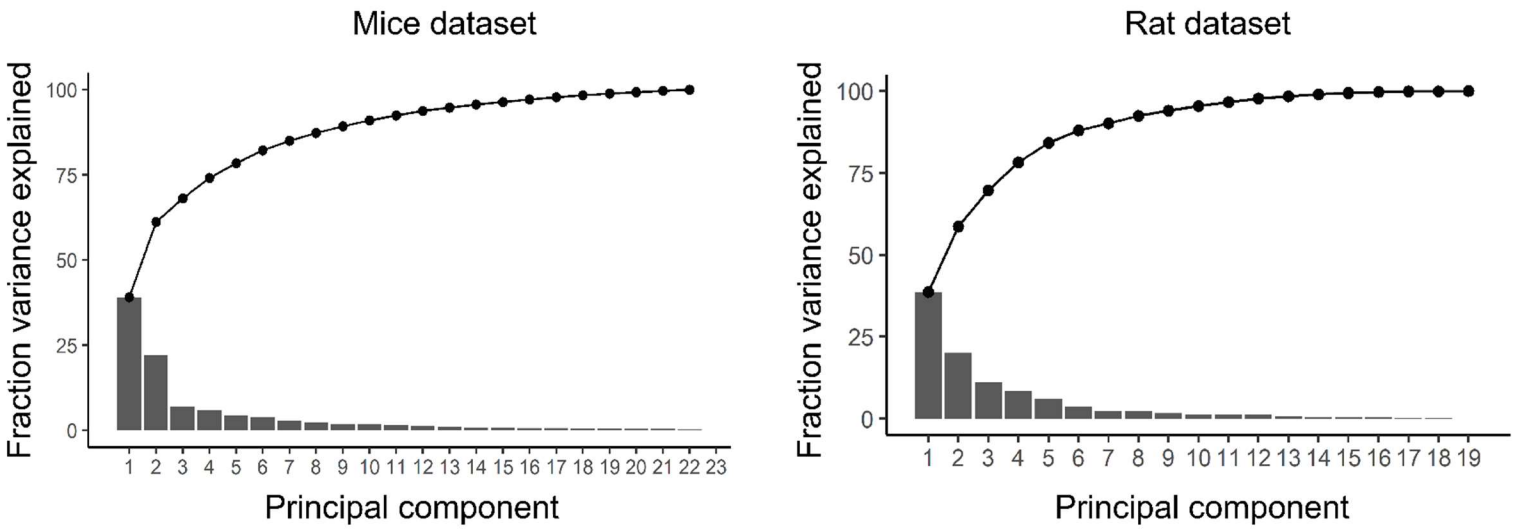

fig. S1- - Principal components of mouse and rat datasets. Principal components, and explained variance from principal component analysis for mouse and rat datasets.

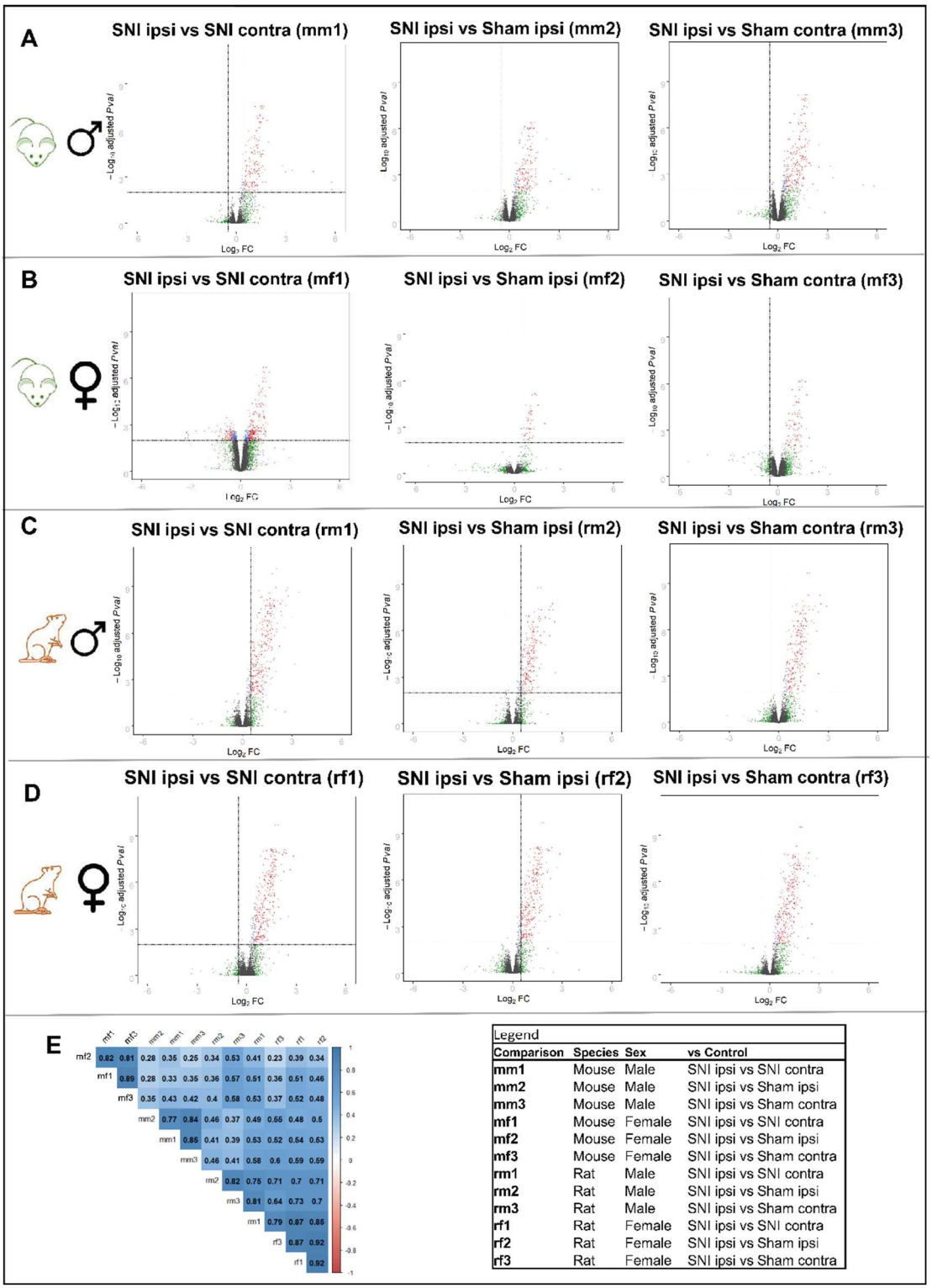

fig. S2- Pairwise comparison of SNI_ipsi vs each of the comparators. (A-D) Volcano plots of twelve pairwise comparisons (A) male mice (B) female mice (C) male rats and (D) female rats. (E) Correlation coefficients by Pearson method between 12 comparisons.

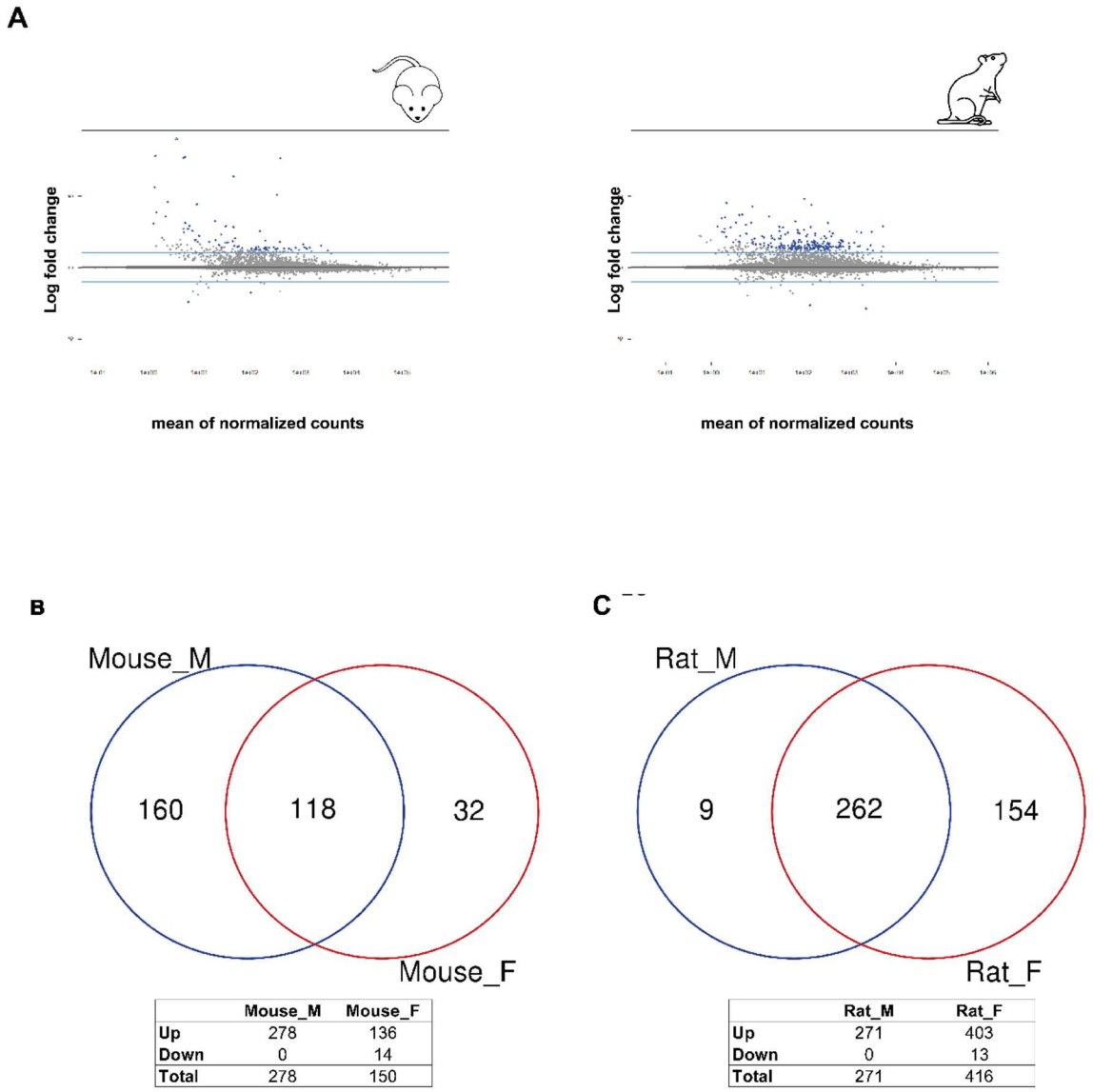

	Mouse_M	Mouse_F
Up	278	136
Down	0	14
Total	278	150

	Rat_M	Rat_F
Up	271	403
Down	0	13
Total	271	416

fig. S3- Overview of differential gene expression in mice and rat datasets. (A) MA plots of injured vs not injured sex combined. (B) Venn diagram shows common DEGs between males and females in mice and (C)Venn diagram for rat.

A

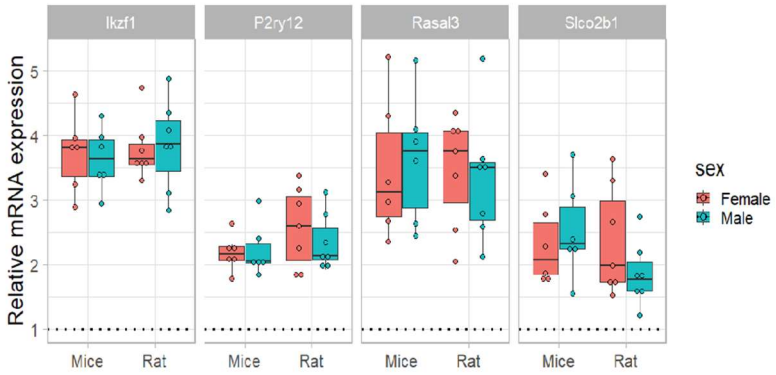
Ikzf1
P2ry12
Rasal3
Slco2b1
Relative mRNA expression
1
2
3
4
5
Mice
Rat
sex
Female
Male

B

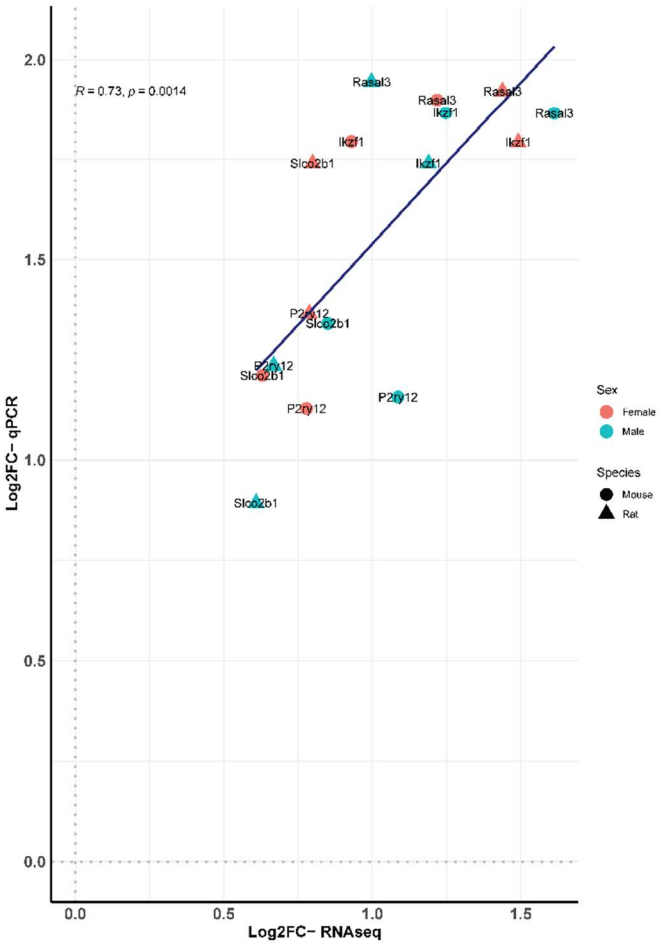
R = 0.73, p = 0.0014
Log2FC− qPCR
Log2FC− RNAseq
0.0
0.5
1.0
1.5
2.0
Rasal3
Ikzf1
Slco2b1
P2ry12
Sex
Female
Male
Species
Mouse
Rat

23

24 fig. S4- RNA-seq validation. (A) mRNA expression of 4 DEGs by qPCR, the delta-delta CT
25 method was used to calculate the fold change vs SNI contra, the values represent the
26 individual animal. (B) Pearson correlation of RNA-seq results and qPCR.
27

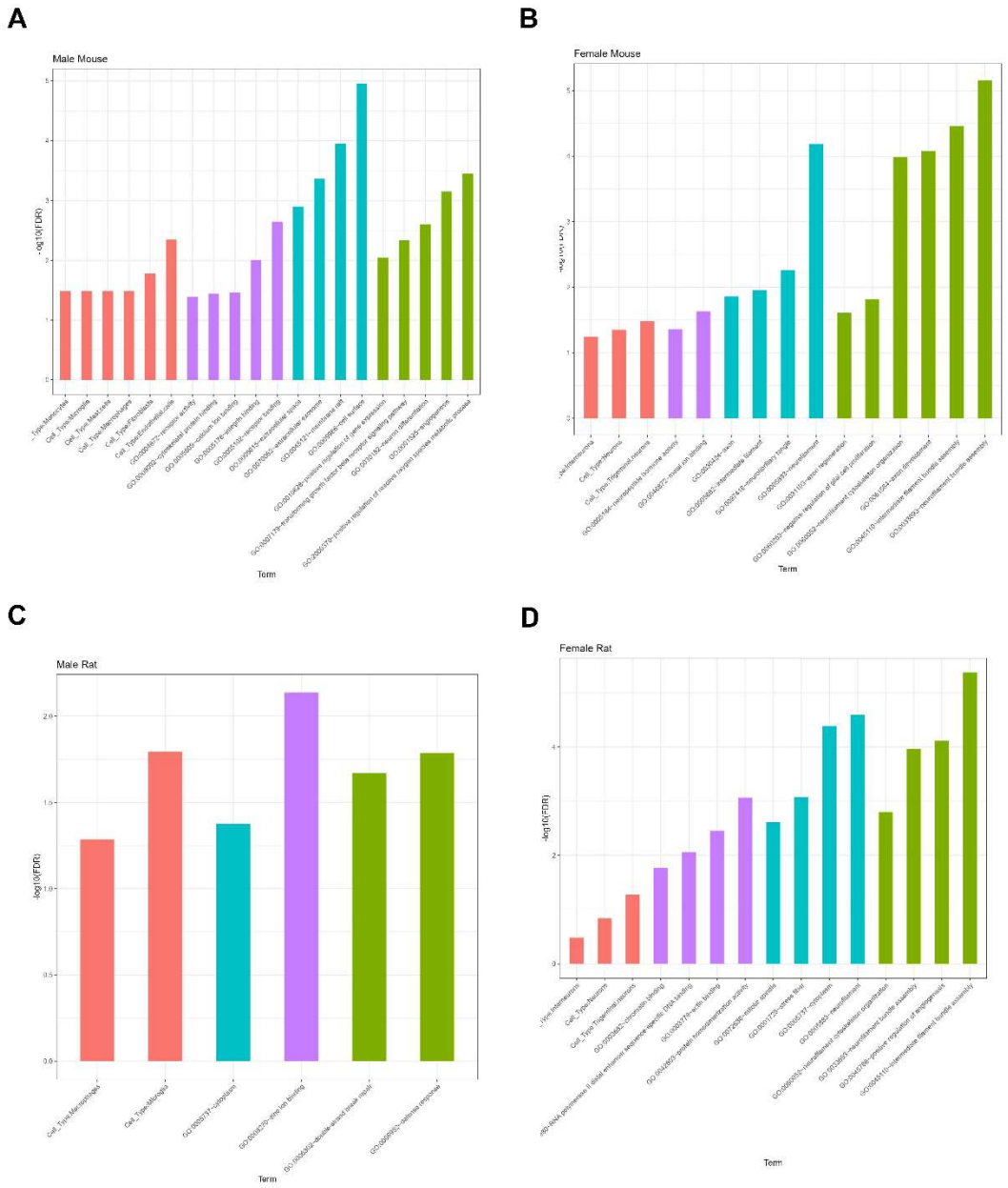

fig. S5- Gene ontology analysis and cell type profile for DEGs exclusive to sex or species. green color represents biological process, blue: cellular component, purple: molecular function is and red color represents cell-deconvolution. (A) male mice, (B) female mice, (C) male rats (D) and female rats.

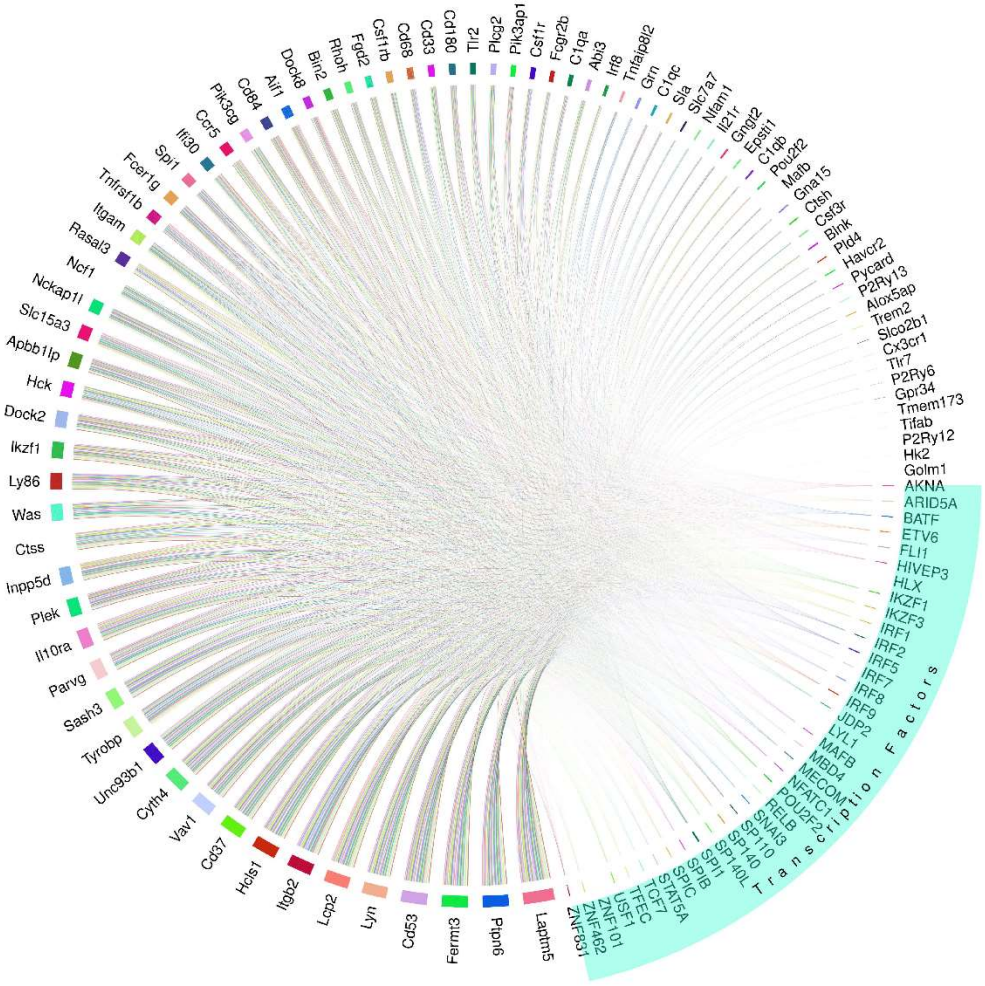

fig. S6- Gene regulation of conserved genes. Circoplot represents transcription factors and their connection with common differentially expressed genes.

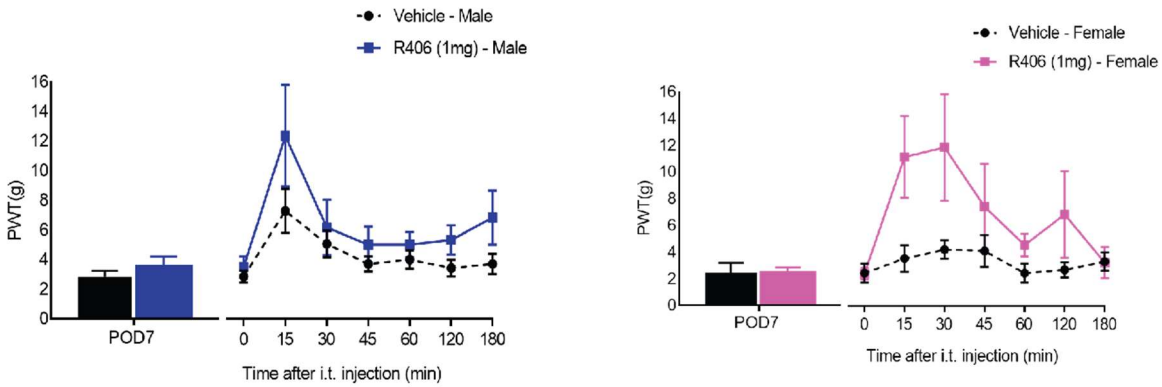

fig. S7- R406 efficacy in male and female rats. Paw withdrawal threshold from von Frey filaments on the ipsilateral side 7 days after surgery in SNI animals, (N=6-7/sex/treatment) and comparing SNI ipsilateral of R406 (1mg) and vehicle.